Continual exit of human cutaneous resident memory CD4 T cells that seed distant skin sites

M.M. Klicznik[1], P.A. Morawski[2], B. Höllbacher[1,2], S. Varkhande[1], S. Motley[2], M.D. Rosenblum[3], T. Duhen[2], D.J. Campbell[2,4*], I.K. Gratz[1,2,5*]

[1] Department of Biosciences, University of Salzburg, Salzburg, Austria

[2] Benaroya Research Institute, Seattle, Washington, USA

[3] Department of Dermatology, University of California, San Francisco, California, USA

[4] Department of Immunology, University of Washington School of Medicine, Seattle, Washington, USA

[5] EB House Austria, Department of Dermatology, University Hospital of the Paracelsus Medical University, Salzburg, Austria

[*] Last authors contributed equally

Contact: campbell@benaroyaresearch.org; iris.gratz@sbg.ac.at

T cell memory is compartmentalized into circulating and tissue-resident cell populations. While circulating memory T cells continually patrol the body via the blood and lymphatics, tissue-resident memory T cells (T_{RM}) persist locally in non-lymphoid tissues, providing a front-line of defense against recurring insults[1]. T_{RM} are abundant at barrier surfaces such as the intestines, lungs, and skin, and are defined by expression of the markers CD103 and/or CD69 which function to retain T_{RM} in these epithelial tissues[2,3]. However, we found that $CD4^+CD69^+CD103^+$ T_{RM} in human skin can downregulate CD69, exit the tissue and be identified as a phenotypically unique population in the circulation. Functionally, these mobilized (m)T_{RM} produce the cytokines IL-22 and IL-13, and RNA sequencing identifies a set of signature genes shared by $CD103^+$ T_{RM} cells in blood and skin consistent with a role in host-defense and tissue-repair responses[4,5]. Studies in skin-humanized mice given full-thickness skin grafts show that after exit from the skin, $CD103^+$ mT_{RM} can migrate to and seed distant tissue sites. Thus, contrary to current models, $CD4^+CD103^+$ T_{RM} in the skin can be mobilized to the circulation, promoting the spread of a functionally specialized T cell population throughout the skin, a large barrier organ, and allowing for isolation and study of these cells from the blood, a widely accessible tissue source.

The skin is an immunologically active barrier organ, and as such is home to a number of specialized T cell populations[6]. Cutaneous T cells are not only important for preventing skin infection, but also can directly participate in tissue repair through production of cytokines that promote epithelial cell proliferation and survival[7,8]. Confirming prior analyses[2], the vast majority of both $CD8^+$ and $CD4^+$ T cells in the skin expressed CD69, and a subset of $CD69^+$ cells also expressed the CD103 integrin and thus had a typical T_{RM} phenotype (Fig. 1a, b). Most of these $CD69^+CD103^+$ T_{RM} also expressed the cutaneous lymphocyte antigen (CLA), a glycan moiety that promotes skin homing of immune cells by acting as a ligand for E-selectin (Fig. 1c)[9], and previous work has shown that $CD69^+$ T_{RM} persist in the skin following depletion of circulating T cells with anti-CD52, indicating that they can be maintained locally and do not require continual replacement by circulating cells from the blood[1]. However, in skin explant cultures we and others found that cutaneous $CD4^+CLA^+$ T cells exited the tissue and could be detected in the culture media[10], and exit was associated with downregulation of CD69 by both $CD103^+$ and $CD103^-$ cells (Fig. 1d). By contrast, very few $CD8^+$ T cells exited the skin in the explant cultures, consistent with continued tissue-residency of this population[11]. Accordingly, analyses of human cutaneous lymph revealed constitutive exit of predominantly $CD4^+$ T cells from the skin[12].

In addition to being found on T_{RM} in the skin, CLA is also present on a subset of circulating $CD45RA^-CD45RO^+$ memory T cells[13]. Exit of $CD4^+$ T_{RM} from our skin explant cultures suggested some of these cells might be mobilized (m)T_{RM} from the tissue that re-entered the circulating pool of CLA^+ memory cells *in vivo*. However, as CD69 is the principle marker used to identify T_{RM}, its downregulation associated with tissue-exit would confound identification of any mT_{RM} in the blood. Therefore, to test whether mT_{RM} cells could be found in the circulation, we performed mass cytometry analysis of peripheral blood mononuclear cells (PBMC) from 5 healthy subjects, focusing on expression of the other principle T_{RM} marker CD103. t-distributed Stochastic Neighbor Embedding (t-SNE) analysis revealed 10 distinct clusters of $CD3^+CD45RA^-CLA^+$ memory T cells present in all subjects examined (Fig. 1e, Extended Data Fig. 1), including 5 distinct clusters of $CD4^+$ T cells (Fig. 1f). Interestingly, the smallest cluster of $CD4^+$ T cells (cluster 10) was characterized by expression of CD103 and its dimerization partner β7 integrin, and also expressed chemokine receptors strongly indicative of skin tropism such as CCR4, CCR6, and CCR10 (Fig. 1f, g). By contrast they did not express markers of central memory T cells (CCR7), regulatory T cells (Foxp3, CD25), T helper (Th)1 cells (CXCR3), Th17 cells (CD161) or natural killer T cells (CD56). The lack of CCR7 expression indicates that these cells are distinct from $CCR7^{int/+}CD69^-CD103^{+/lo}$ cells that undergo CCR7-dependent migration from

the skin to the draining lymph nodes in mice[14], and from the CCR7$^+$CD62L$^-$ migratory memory (T_{MM}) cells described in human skin[2].

Using conventional flow cytometry we confirmed the presence of circulating CD45RA$^-$ CD4$^+$CLA$^+$CD103$^+$ memory T cells, and compared their abundance and phenotype to CD103$^+$ T_{RM} cells in the skin (Fig. 2a, b). Although CLA$^+$CD103$^+$ memory T cells are common in the skin (26 +/- 9% of CD4$^+$CLA$^+$ T cells), they are a rare population in the blood, representing on average <2% of CLA$^+$ circulating CD45RA$^-$ memory T cells, and <0.2% of total CD4$^+$ T cells (Fig. 2c, Extended Data Fig. 2). CLA$^+$CCR7$^+$CD103$^-$ cells showed a reciprocal distribution in skin and blood, whereas the bulk of CD4$^+$CLA$^+$ T cells in both tissues were CCR7$^-$CD103$^-$. CLA$^+$CD103$^+$ T_{RM} in the skin shared the CCR4$^+$CCR6$^+$CXCR3$^-$ chemokine receptor profile with circulating CLA$^+$CD103$^+$ memory T cells, and CLA$^+$CD103$^+$ cells in the blood and all populations in the skin were low for expression of CD49d (α4 integrin), which like CD103 can pair with β7 integrin, and in this combination promotes T cell localization to the intestinal mucosa (Fig. 2d)[15]. Similarly, like skin T_{RM}, CLA$^+$CD103$^+$ cells in the blood were CD27^{lo} indicating that they are terminally differentiated[16], whereas most circulating CLA$^+$CD103$^-$CCR7$^{+/-}$ memory T cells were CD27$^+$. Additionally, significant fractions of circulating CLA$^+$CD103$^+$ memory T cells expressed the markers CD101 and CD9, which were also expressed by most CD103$^+$ T_{RM} in the skin. CD101 was recently identified as a marker of CD8$^+$CD103$^+$ T_{RM} in various human tissues[3], whereas CD9 is highly expressed by keratinocytes and T cells in the skin, where it modulates TGF-β signaling, integrin function, cell migration, and wound healing[17,18]. However, consistent with downregulation of CD69 by T cells that migrate out of the skin *in vitro*, CLA$^+$CD103$^+$ cells in the blood were almost all CD69$^-$ (Fig. 2e). Functionally, we compared cytokine production by CLA$^+$ T cells from skin and blood following *ex vivo* stimulation and intracellular cytokine staining. CD103$^+$CLA$^+$ cells from both organs produced the cytokines IL-22 and IL-13, but were largely negative for IFN-γ or IL-17A (Fig. 2f-i and Extended Data Fig. 3). This cytokine phenotype is consistent with that of Th22 cells[19,20], and distinguished CLA$^+$CD103$^+$ T cells from other populations of CD103$^-$ T cells in both tissues. Thus, these represent a phenotypically distinct and functionally specialized T cell population.

To assess the transcriptional signature of circulating and skin-resident CLA$^+$CD103$^+$ T cells, we performed RNA-seq on sorted CLA$^+$ T cell populations from blood and skin (Extended Data Fig. 4). Analysis of blood cells identified a unique 83-gene signature of CLA$^+$CD103$^+$ T cells that distinguished them from other circulating CLA$^+$ memory T cells, and that was also significantly enriched in CD103$^+$ vs. CD103$^-$ skin T_{RM} (Fig. 3a). Hierarchical clustering based on these genes grouped CLA$^+$CD103$^+$ T cells from blood with CLA$^+$CD103$^+$ T_{RM} from skin, consistent with the notion that circulating CLA$^+$CD103$^+$ cells represent mT_{RM} (Fig. 3b), and principle component analysis based on these genes clearly separated skin T_{RM} and circulating CLA$^+$CD103$^+$ cells from circulating CLA$^+$CD103$^-$CCR7$^{+/-}$ memory T cells (Fig. 3c). Moreover, when applied to publicly available transcriptional profiles of human CD4$^+$ T cells, the CD103$^+$ gene signature (derived solely from CLA$^+$CD103$^+$ T cells in the blood) distinguished CD69$^+$ T_{RM} from CD69$^-$ cells in both lung and spleen, further supporting a transcriptional link between circulating CLA$^+$CD103$^+$ cells and tissue T_{RM} (Fig. 3d).

CD103 expression by T_{RM} is induced upon migration into non-lymphoid sites by tissue-derived factors including TGF-β[21]. Consistent with this, several TGF-β related genes are upregulated in circulating and skin-resident CLA$^+$CD103$^+$ cells as part of their unique gene signature (Fig. 3e and Extended Data Fig. 5). Moreover, along with *ITGAE* (the gene encoding CD103)*, CD27* and *CD101*[3], we found several additional T_{RM}-associated genes differentially expressed by circulating CLA$^+$CD103$^+$ cells, including *CCR8*[22]*, CXCR6*[3]*, EOMES*[23] *and PPARG*[24]. We also identified overlapping functional modules of genes differentially expressed by circulating CLA$^+$CD103$^+$ T cells that control cellular migration and adhesion, modulate host defense and tissue inflammation, and promote tissue-repair and barrier function (Fig. 3e,

Extended Data Fig. 5). In this last context, it is important to note that IL-22 acts directly on keratinocytes to promote their survival, proliferation, migration and anti-microbial functions[5], whereas IL-13 activates cutaneous fibroblasts and promotes M2 macrophage differentiation and wound healing[25], indicative of a role for CLA^+CD103^+ T cells in promoting normal tissue homeostasis and repair in the skin. Accordingly, CLA^+CD103^+ cells in the blood and skin also expressed the receptor components for the epithelial-derived cytokine IL-25 (*IL17RA, IL17RB)*, indicating that they have the ability to sense and respond directly to keratinocytes that produce IL-25 upon tissue damage or cellular stress[26]. Taken together with our phenotypic and functional analyses, the transcriptional profile of blood CLA^+CD103^+ T cells is consistent with their origin and function within the skin, a TGF-β-rich barrier site exposed to microbial threats and frequent tissue damage.

To directly test the hypothesis that CLA^+CD103^+ T_{RM} can exit the skin and seed distant tissue sites via the circulation *in vivo*, we used a humanized mouse model in which full thickness human skin was grafted onto immunodeficient NOD, scid, common-γ chain-deficient (NSG) mice[27]. Some of these recipients also carried engineered skin (ES) grafts generated from cultured human keratinocytes and fibroblasts using a grafting chamber system in which spontaneous cell sorting creates organotypic ES that closely resembles human skin[28] (Fig. 4a,b, Extended Data Fig 6). Importantly, the ES grafts were initially devoid of any immune cells, and since no PBMC were transferred into these animals the only potential source of human T cells were the skin grafts. Five to eight weeks after skin grafting, $CD4^+CLA^+$ T cells had exited the grafts and were evident in both the spleens (8/10) and ES (4/6) of the recipient animals, and among these were CLA^+CD103^+ (Fig 4c,d). By contrast, no human cells were found in adjacent murine skin (Extended Data Fig. 7). CLA^+CD103^+ T cells were low for CD27 in all tissues and, similar to what we observed in human blood, CD9 and CD69 were downmodulated on cells that exited the skin and were found in the spleen but re-expressed by cells entering the ES (Fig. 4e). Importantly, expression of CD103 is not simply an artifact of the xenogenic system we use, as we did not observe induction of CD103 by $CD4^+$ T cells in NSG mice upon transfer of total PBMC (Extended Data Fig. 8). Instead, these data demonstrate that skin-resident CLA^+CD103^+ T_{RM} can downregulate CD69, become mobilized from the skin, enter the circulating T cell pool, and re-seed a distant skin site.

$CD69^+$ T_{RM} have been defined as non-circulating cells that mediate optimal protective responses to site-specific challenges through rapid activation of an immune response *in situ*[29,2]. However, it was recently reported that murine $CD8^+$ memory T cells could exit the skin and become resident in draining lymphoid organs, and these cells shared phenotypic and transcriptional signatures with tissue T_{RM}[30]. We now demonstrate tissue exit of human cutaneous $CD4^+$ T_{RM}, and identify $CD103^+$ mT_{RM} as a phenotypically and functionally distinct population of circulating T cells. Although mobilization of T_{RM} from the skin to seed distant sites appears to contradict the idea that T_{RM} are maintained locally in the tissue long-term, it is important to note that when we combine the frequency of circulating $CD103^+$ mT_{RM} and skin T_{RM} with estimates of T cell numbers in human skin and blood[9], mT_{RM} make up just 0.6% of all CLA^+CD103^+ memory cells in the body at any given time (Extended Data Table 1). However, mobilization, either stochastic or actively triggered, of a fraction of T_{RM} might support the distribution of immunity in a large barrier organ such as the skin as well as provide a reservoir or circulating T cells that could be rapidly recruited to damaged tissue to promote host-defense and tissue-repair.

Acknowledgements
This work was supported by the Focus Program “ACBN” of the University of Salzburg, Austria, NIH grant R01AI127726 awarded to IKG and DJC. MK was recipient of a DOC Fellowship of the Austrian Academy of Sciences. We thank Dr. A. Sir and Dr. R. Reitsamer of the Breast Center of the University Hospital Salzburg, Paracelsus Medical University Salzburg, Austria for

providing us with skin and blood samples. We also thank the flow core personnel (Dr. Gabriele Brachtl, Anna Hochreiter, MSc, Anna Raninger, MSc) of the group of Prof. Dirk Strunk at the Paracelsus Medical University of Salzburg. We thank Dr. Stefan Hainzl, EB House Austria, Department of Dermatology, University Hospital of the Paracelsus Medical University Salzburg, Austria, for the immortalization of primary human keratinocytes and fibroblasts. In Seattle, we thank Kassidy Benoscek and Florence Roan for help in obtaining skin and blood samples, Thien Son-Nguyen for frozen PBMC, Alice Long and Alice Weidemann for help with CyTOF, Vivian Gersuk for help with RNA-seq, and Scott Presnell, Matt Dufort and Hannah DeBerg for helpful discussions on RNA-seq analysis.

Author contributions: M.M.K., P.A.M., B.H., S.V., T.D., D.J.C. and I.K.G. designed the experiments; M.M.K., M.D.R. and I.K.G. developed xenografting methods; M.M.K., P.A.M., B.H., S.V., S.M. and T.D. performed experiments; B.H. performed computational analysis; D.J.C. and I.K.G. wrote the manuscript; M.M.K., P.A.M., B.H., S.V., S.M., T.D. and M.D.R. reviewed and edited the paper; D.J.C. and I.K.G. supervised the project.

Competing interests: None

Figure legends

Figure 1: CD103$^+$CD4$^+$ T cells exit the skin and constitute a unique cell type in human blood. a, Representative flow cytometry analysis of CD69 and CD103 expression by gated CD8$^+$ and CD4$^+$ T cells from human skin. **b**, Graphical summary of the proportions of CD69$^+$CD103$^+$, CD69$^+$CD103$^-$ and CD69$^-$CD103$^-$ T cells among CD8$^+$ and CD4$^+$ skin T cells. **c**, Representative flow cytometry analysis of CLA expression by gated CD103$^+$CD69$^+$ T_{RM} in human skin. **d**, Human skin was adhered to tissue culture plates and cultured for 7 days submerged in media. The ratio of CD4$^+$ and CD8$^+$ T cells and the expression of CLA and CD103 by T cells in the indicated samples were analyzed by flow cytometry. Representative data (N=2) **e**, (Top), Mass cytometry analysis of CD45RA and CLA expression by gated CD3$^+$CD45$^+$ PBMC showing the gate used to define CD3$^+$CLA$^+$ T cells for subsequent clustering analysis. (Bottom), tSNE analysis and clustering of CD3$^+$CLA$^+$ T cells from blood of 5 healthy donors based on expression of CD4, CD8, CCR7, CD103, β7Integrin, CXCR3, CCR6, CCR4, CCR10, Foxp3, CD27, β7 integrin, CD25, CD161, and CD56. **f,** Heat map showing relative expression of the indicated markers in each of the CD3$^+$CLA$^+$ cell clusters. **g**, tSNE analysis of CD3$^+$CLA$^+$ T cells overlaid with relative expression of the indicated markers.

Figure 2: Shared phenotype and function of CD103$^+$ CLA$^+$ T cells from human blood and skin. a, Representative flow cytometry analysis of CD45RA and CLA expression by gated CD4$^+$ T cells from blood and skin of healthy donors. **b**, Representative flow cytometry analysis of CCR7 and CD103 expression by gated CD4$^+$CD45RA$^-$CLA$^+$ memory T cells from PBMC and skin of healthy donors. **c**, Graphical summary of the proportions of CCR7$^+$CD103$^-$, CCR7$^-$CD103$^-$, and CCR7$^-$CD103$^+$ T cells among CD4$^+$CD45RA$^-$CLA$^+$ T cells from blood and skin. **d,e**, Representative flow cytometry analysis and graphical summary of expression of the indicated markers by CD4$^+$ T cell populations in the blood and skin as indicated. **f,g,h,i,** Graphical summary of the proportions of CLA$^-$CD103$^-$, CLA$^+$CD103$^-$, and CLA$^+$CD103$^+$ CD4$^+$CD45RA$^-$ cells producing IL-22, IL-13, IFN-γ, and IL-17A as indicated upon *ex vivo* stimulation with PMA/ionomycin and intracellular cytokine staining. Significance determined by one-way repeated measures ANOVA with Tukey's post-test for pairwise comparisons, *p <0.05.

Figure 3: CD103$^+$ CLA$^+$ T cells from human blood and skin share a transcriptional profile. Whole transcriptome profiling by RNA-sequencing was performed on sorted CLA$^+$ T cell subsets from blood or skin. **a**, (top) Venn diagram showing the number of significantly differentially expressed (DE) genes (FDR<0.05 and log2 fold-change >1) between CLA$^+$CD103$^+$ T cells and either CLA$^+$CD103$^-$CCR7$^+$ or CLA$^+$CD103$^-$CCR7$^-$ T cells as indicated. The overlapping 83 genes were designated the CD103$^+$ gene signature (bottom). Barcode plot showing the distribution of the CD103$^+$ signature genes (red=up- blue=down-regulated in CD103$^+$) relative to gene expression changes comparing CD103$^+$ and CD103$^-$CCR7$^-$ T cells from the blood or skin as indicated. Significance determined by rotation gene set tests. **b**, Heat map and hierarchical clustering of RNA-seq samples from the indicated blood and skin cell populations based on the CD103$^+$ gene signature. **c**, PCA analysis of RNA-seq samples from the indicated blood and skin cell populations based on the CD103$^+$ gene signature or on 83 randomly selected genes. **d**, PCA analysis of RNA-seq samples from CD4$^+$CD69$^+$ and CD4$^+$CD69$^-$ T cell populations from lung and spleen (data from GEO dataset GSE94964[3]) based on the CD103$^+$ gene signature or 83 randomly selected genes. **e**, Venn diagram showing functional annotation of key genes up- or down-regulated by CLA$^+$CD103$^+$ T cells in blood or skin identified in our phenotypic, functional, and transcriptional analyses.

Figure 4: CD103$^+$CLA$^+$ T_{RM} can exit the skin and reseed distant skin sites in a xenograft model. a, Experimental schematic for production of engineered skin (ES) followed by

xenografting full-thickness human skin onto NSG mice. **b**, Representative photograph of ES and skin grafts on day 145. **c**, Representative flow cytometry analysis and **d,** graphical summary of CLA and CD103 expression by live gated human $CD45^{+}CD3^{+}CD4^{+}CD45RA^{-}$ T cells from skin grafts (5-8 weeks), spleen (5-8 weeks), and ES (5 weeks after skin grafting). Open, filled and half-filled symbols denote samples derived from 3 different skin donors. **e**, Representative flow cytometry analysis and graphical summary of expression of CD27, CD9 and CD69 by gated $CD45^{+}CD4^{+}CD45RA^{-}CD103^{+}CLA^{+}$ T cells in the skin grafts, spleen, and ES 5-8 weeks after skin grafting (day 145 relative to ES generation). Significance determined by one-way ANOVA with Tukey's post-test for pairwise comparisons, *$p < 0.05$.

References

1. Clark, R. A. *et al.* Skin effector memory T cells do not recirculate and provide immune protection in alemtuzumab-treated CTCL patients. *Sci Transl Med* **4,** 117ra7 (2012).
2. Watanabe, R. *et al.* Human skin is protected by four functionally and phenotypically discrete populations of resident and recirculating memory T cells. *Sci Transl Med* **7,** 279ra39 (2015).
3. Kumar, B. V. *et al.* Human tissue-resident memory T cells are defined by core transcriptional and functional signatures in lymphoid and mucosal sites. *Cell Rep* **20,** 2921–2934 (2017).
4. Eyerich, S. *et al.* Th22 cells represent a distinct human T cell subset involved in epidermal immunity and remodeling. *J. Clin. Invest.* **119,** 3573–3585 (2009).
5. Sonnenberg, G. F., Fouser, L. A. & Artis, D. Border patrol: regulation of immunity, inflammation and tissue homeostasis at barrier surfaces by IL-22. *Nat. Immunol.* **12,** 383–390 (2011).
6. McCully, M. L. & Moser, B. The human cutaneous chemokine system. *Front Immunol* **2,** 33 (2011).
7. Havran, W. L. & Jameson, J. M. Epidermal T cells and wound healing. *J. Immunol.* **184,** 5423–5428 (2010).
8. Toulon, A. *et al.* A role for human skin–resident T cells in wound healing. *J Exp Med* **206,** 743–750 (2009).
9. Clark, R. A. *et al.* The vast majority of CLA+ T cells are resident in normal skin. *J. Immunol.* **176,** 4431–4439 (2006).
10. Clark, R. A. *et al.* A novel method for the isolation of skin resident T cells from normal and diseased human skin. *J. Invest. Dermatol.* **126,** 1059–1070 (2006).
11. Gebhardt, T. & Mackay, L. K. Local immunity by tissue-resident CD8(+) memory T cells. *Front Immunol* **3,** 340 (2012).
12. Yawalkar, N., Hunger, R. E., Pichler, W. J., Braathen, L. R. & Brand, C. U. Human afferent lymph from normal skin contains an increased number of mainly memory / effector CD4(+) T cells expressing activation, adhesion and co-stimulatory molecules. *Eur. J. Immunol.* **30,** 491–497 (2000).
13. Fuhlbrigge, R. C., Kieffer, J. D., Armerding, D. & Kupper, T. S. Cutaneous lymphocyte antigen is a specialized form of PSGL-1 expressed on skin-homing T cells. *Nature* **389,** 978–981 (1997).
14. Bromley, S. K., Yan, S., Tomura, M., Kanagawa, O. & Luster, A. D. Recirculating memory T cells are a unique subset of CD4+ T cells with a distinct phenotype and migratory pattern. *J. Immunol.* **190,** 970–976 (2013).
15. Berlin, C. *et al.* Alpha 4 beta 7 integrin mediates lymphocyte binding to the mucosal vascular addressin MAdCAM-1. *Cell* **74,** 185–195 (1993).
16. Fritsch, R. D. *et al.* Stepwise differentiation of CD4 memory T cells defined by expression of CCR7 and CD27. *J. Immunol.* **175,** 6489–6497 (2005).
17. Reyes, R., Cardeñes, B., Machado-Pineda, Y. & Cabañas, C. Tetraspanin CD9: A Key Regulator of Cell Adhesion in the Immune System. *Front Immunol* **9,** 863 (2018).
18. Zhang, J. *et al.* CD9 is critical for cutaneous wound healing through JNK signaling. *J. Invest. Dermatol.* **132,** 226–236 (2012).
19. Duhen, T., Geiger, R., Jarrossay, D., Lanzavecchia, A. & Sallusto, F. Production of interleukin 22 but not interleukin 17 by a subset of human skin-homing memory T cells. *Nat. Immunol.* **10,** 857–863 (2009).
20. Trifari, S., Kaplan, C. D., Tran, E. H., Crellin, N. K. & Spits, H. Identification of a human helper T cell population that has abundant production of interleukin 22 and is distinct from T(H)-17, T(H)1 and T(H)2 cells. *Nat. Immunol.* **10,** 864–871 (2009).
21. Mackay, L. K. *et al.* The developmental pathway for CD103(+)CD8+ tissue-resident

memory T cells of skin. *Nat. Immunol.* **14,** 1294–1301 (2013).
22. McCully, M. L. *et al.* CCR8 Expression Defines Tissue-Resident Memory T Cells in Human Skin. *J. Immunol.* **200,** 1639–1650 (2018).
23. Mackay, L. K. *et al.* T-box Transcription Factors Combine with the Cytokines TGF-β and IL-15 to Control Tissue-Resident Memory T Cell Fate. *Immunity* **43,** 1101–1111 (2015).
24. Pan, Y. *et al.* Survival of tissue-resident memory T cells requires exogenous lipid uptake and metabolism. *Nature* **543,** 252–256 (2017).
25. Ferrante, C. J. & Leibovich, S. J. Regulation of Macrophage Polarization and Wound Healing. *Adv Wound Care (New Rochelle)* **1,** 10–16 (2012).
26. Xu, M. *et al.* An Interleukin-25-Mediated Autoregulatory Circuit in Keratinocytes Plays a Pivotal Role in Psoriatic Skin Inflammation. *Immunity* **48,** 787-798.e4 (2018).
27. King, M. *et al.* A new Hu-PBL model for the study of human islet alloreactivity based on NOD-scid mice bearing a targeted mutation in the IL-2 receptor gamma chain gene. *Clin. Immunol.* **126,** 303–314 (2008).
28. Wang, C. K., Nelson, C. F., Brinkman, A. M., Miller, A. C. & Hoeffler, W. K. Spontaneous cell sorting of fibroblasts and keratinocytes creates an organotypic human skin equivalent. *J. Invest. Dermatol.* **114,** 674–680 (2000).
29. Steinert, E. M. *et al.* Quantifying Memory CD8 T Cells Reveals Regionalization of Immunosurveillance. *Cell* **161,** 737–749 (2015).
30. Beura, L. K. *et al.* T Cells in Nonlymphoid Tissues Give Rise to Lymph-Node-Resident Memory T Cells. *Immunity* **48,** 327-338.e5 (2018).

METHODS

Human specimens. Normal human skin was obtained from patients undergoing elective surgery, in which skin was discarded as a routine procedure. Blood and/or discarded healthy skin was donated upon written informed consent at the University Hospital Salzburg, Austria, or the Virginia Mason Medical Center in Seattle, WA, USA.

Mice. All animal studies were approved by the Austrian Federal Ministry of Science, Research and Economy. NOD.Cg-Prkdcscid Il2rgtm1Wjl/SzJ (NSG) mice were obtained from The Jackson Laboratory and bred and maintained in a specific pathogen-free facility in accordance with the guidelines of the Central Animal Facility of the University of Salzburg.

Skin explant cultures. Skin was washed in PBS with 1% Pen/Strep and 0.1% Primocin (Invivogen; ant-pm-1) for 5 minutes. Small pieces of 1-2mm of split-skin were generated using forceps and sharp scissors. Pieces were placed in 60mm dish and allowed to adhere for 10 minutes. Crawl-out medium consisting of 50% Epilife (Gibco, MEPICF500) and 50% RPMI-complete (RPMIc: RPMI 1640 (Gibco; 31870074) with 5% human serum (Sigma-Aldrich; H5667 or H4522), 1% penicillin/streptomycin (Sigma-Aldrich; P0781), 1% L-Glutamine (Gibco; A2916801), 1%NEAA (Gibco; 11140035), 1% Sodium-Pyruvate (Sigma-Aldrich; S8636) and 0.1% β-Mercaptoethanol (Gibco; 31350-010)) containing 20 U/ml IL-2 (Immunotools; 11340023) was added to explant cultures. Seven days later, cells in culture medium were analyzed by flow cytometry.

Cytometry by time-of-flight (CyTOF). Human frozen PBMCs were thawed and rested for 12-15h. The samples were washed with Ca- and Mg-free PBS (Sigma; D8537) and stained with 50µM Cisplatin (Enzo Life Sciences; ALX-400-040-M250) in PBS for 1 minute to exclude dead cells. The cells were washed and resuspended with Human TruStain FcX (Biolegend; 422302) for five minutes before adding the primary surface staining cocktail for 20m, washing and staining with the secondary surface cocktalk for 20m. Intrcellular staining was performed following fixation and permeabalization using the Maxpar Nuclear Antigen Staining Buffer Set (Fluidigm; 201063) for 60 minutes, after which cells were incubated overnight at 4°C with Maxpar Fix and Perm Solution containing 125nM Cell-ID Intercalator-Ir (Fluidigm; 201192A) for DNA staining. Cells were washed with MilliQ H_20 and resuspended in MilliQ H_20 spiked with 1/20th Maxpar EQ Four Element Calibration Beads (Fluidigm; 201078) to a density of <500.000 cells/mL. Data was acquired on a CyTOF 1.5 (Fluidigm) instrument. For analysis, FCS files on gated CD3+CLA+ cells were generated using FlowJo software (Tree Star, inc.). t-distributed Stochastic Neighbor Embedding (t-SNE) analysis was performed in R using the cytofkit R package, and clustering was performed with FlowSOM.

T cell isolation from skin for flow cytometry and RNAseq. Tissues were minced and digested using collagenase type 4 and DNAse as previously described[1]. Briefly, subcutaneous fat was removed before skin was minced with dissection scissors and surgical scalpel. Approximately 1cm^2 of skin was digested overnight in 5%CO_2 at 37°C with 3ml of digestion mix containing 0.8mg/ml Collagenase Type 4 (Worthington; #LS004186) and 0.02mg/ml DNAse (Sigma-Aldrich; DN25) in RPMIc. Samples were filtered, washed with RPMI and PBS and stained for flow cytometry/cell sorting or stimulated for intracellular cytokine staining.

PBMC isolation for flow cytometry and RNAseq. Human PBMCs were isolated using Ficoll-Hypaque (GE-Healthcare; GE17-1440-02) gradient separation. For RNAseq $CD4^+$ T cells were enriched using CD4 microbeads (Miltenyi; 130-045-101) and $4x10^6$ cells/ml were resuspended in RPMIc with 50 U/ml IL-2 (Immunotools; 11340023) in a 24-well and stimulated for 20h with 25µl/ml ImmunoCult CD3/CD28 T cell activator (Stemcell; 10971) prior to staining and cell sorting.

Flow cytometry. For FACS-sorting cells were stained in FACS buffer (PBS + 1 % FBS +1 mM EDTA) for surface markers. For detection of intracellular cytokine production, skin single cell suspensions and PBMCs were stimulated with 50 ng/ml PMA (Sigma-Aldrich; P8139) and 1 µg/ml Ionomycin (Sigma-Aldrich; I06434) with 10 µg/ml Brefeldin A (Sigma-Aldrich; B6542) for 3.5 hrs. For permeabilization and fixation Cytofix/Cytoperm kit was used (BectonDickinson; RUO 554714). Data were acquired on LSR Fortessa, LSRII (both BD Biosciences) or Cytoflex LS (Beckman.Coulter) flow cytometers and analyzed using FlowJo software (Tree Star, Inc.)

Illumina sequencing. 500 cells per population were sorted into lysis buffer using a BD FACSARIA III or FACSFUSION instruments (BD Biosciences), and cDNA was prepared using the SMART-Seq v4 Ultra Low Input RNA Kit for Sequencing (Takara). Library construction was performed using the NexteraXT DNA sample preparation kit (Illumina) using half the recommended volumes and reagents. Dual-index, single-read sequencing of pooled libraries was run on a HiSeq2500 sequencer (Illumina) with 58-base reads and a target depth of 5 million reads per sample. Base-calling and demultiplexing were performed automatically on BaseSpace (Illumina) to generate FASTQ files.

RNAseq analysis. The FASTQ files were processed in order to remove reads of zero length (fastq_trimmer v.1.0.0), remove adapter sequences (fastqmcf tool v.1.1.2) and perform quality trimming from both ends until a minimum base quality ≥ 30 (FASTQ quality trimmer tool v.1.0.0). Reads were aligned to the human reference genome (build hg38) with TopHat (v.1.4.0) and read counts per Ensembl gene ID were quantified with htseq-count (v.0.4.1). Quality metrics for the FASTQ and BAM/SAM files were generated with FastQC (v.0.11.3) and Picard (v.1.128). Processing of FASTQ and BAM/SAM files was executed on the Galaxy workflow platform of Globus genomics. Statistical analysis of gene expression was assessed in the R environment (v.3.4.4). Samples with a total number of fastq reads below 1*10^6, mapped reads below 70% or median CV coverage > 1 were excluded from further analysis. Mapping Ensembl Gene IDs to HGNC gene symbols was achieved through biomaRt (GRCh38.p10). Genes were filtered for protein coding genes and those with an expression of CPM > 2 in at least 10% of the libraries. A linear model for gene expression was fit to the filtered 12293 genes using limma (v3.34.9), considering donor effects through a random factor. For visualizations the random effect of the model was approximated by removing the donor effect from the expression data with limma::removeBatchEffect. Genes found to be significantly different (adj.p.val < 0.05 and logFC>2) between $CD103^+$ cells and $CD103^-$ $CCR7^+$ cells as well as between $CD103^+$ cells and $CD103^-CCR7^-$ cells in the blood were defined as the $CD103^+$ gene signature. Enrichment of the $CD103^+$ gene signature in the ranked list of $CD103^+$ cells vs $CD103^-CCR7^-$ cells in the skin was visualized with limma::barcodeplot and quantified with limma::roast. Publicly available data on human $CD4^+$ Tissue-Resident Memory T Cells was retrieved from GEO dataset GSE94964. Gene names were lifted over from hg19 to hg38 nomenclature, the limma::voom transformed expression values were corrected for donor effect with sva::ComBat and PCA was performed on genes from the $CD103^+$ signature or the same number of randomly selected genes.

Generation of engineered skin (ES). Human keratinocytes and fibroblasts were isolated from a normal human skin and immortalized using human papilloma viral oncogenes E6/E7 HPV as previously described[2]. These were cultured in Epilife (Gibco, MEPICF500) and DMEM (Gibco; 11960-044) containing 2% L-Glutamine, 1% Pen/Strep, 10% FBS, respectively. For transplantation, 80% confluent cells were trypsinized (TrypLE express, Gibco; 12604021) washed with PBS and counted. Per mouse, 1-2x10^6 keratinocytes were mixed 1:1 with autologous fibroblasts in 400µl MEM(Gibco; 11380037) containing 1% FBS, 1% L-Glutamine and 1% NEAA were used for *in vivo* generation of engineered skin as described[3].

Transplantation of full thickness skin. 8mm punch biopsies of human full thickness skin were trimmed to an average thickness of 0.5-1mm. Transplants were soaked in PBS + 1%

Pen/Strep + 0.1% Primocin (Invitrogen; ant-pm-1) for 5 minutes and kept on ice in a sterile container with PBS soaked gauze until transplantation. Mice were anesthetized and full thickness wound bed prepared using surgical scissors. Three grafts/mouse were placed on the back and fixed using surgical skin glue (Histoacryl; BRAUN). Transplants were covered with paraffin gauze dressing and bandaged with self-adhesive wound dressing. Bandages were removed after 7 days.

Tissue preparation from mice. Mice were euthanized using CO_2 asphyxiation followed by cervical dislocation. Single cell suspensions were generated from spleen, engineered skin and full thickness grafts and leukocytes analyzed by flow cytometry.

Data availability. Raw and processed RNA-seq data can be found in Extended Data Excel Files 1 and 2

Statistical analysis. Statistical significance of data was calculated with Prism 6.0 software (GraphPad). For comparison between more than two groups statistical analysis was performed using a one-way ANOVA with Tukey's multiple comparisons test. Error bars indicate mean + standard deviation. * denotes adjusted P values ≤ 0.05.

Detailed list of antibodies and reagents can be found in Extended data table 2

Extended Data Methods

Histological staining of skin sections. Normal human skin, engineered skin grafts and adjacent murine skin was excised and frozen in TissueTek (Hartenstein; TTEK). 9 µm cryosections were stained with Hemalum solution acid (Carl Rorth; T865.1) and Eosin Y aqueous solution (Sigma, 201192A). Human type VII collagen was stained by immunofluorescence using anti-human type VII collagen antibody (anti-NC-1 domain of type VII collagen (LH7.2) kindly provided by Dr. Alexander Nyström, University of Freiburg, Germany) and goat anti-rabbit A488 (ThermoFisher; A11008) secondary antibody, and nuclear DAPI staining (ProLong™ Gold Antifade Mountant with DAPI, Invitrogen; P36931).

T cell isolation from murine skin for flow cytometry. Approx. 3 cm^2 of shaved dorsal mouse skin were harvested and single cell suspensions prepared as in[4] and stained for flow cytometry.

References for Methods:

1. Sanchez Rodriguez, R. *et al.* Memory regulatory T cells reside in human skin. *J. Clin. Invest.* **124,** 1027–1036 (2014).
2. Merkley, M. A. *et al.* Large-scale analysis of protein expression changes in human keratinocytes immortalized by human papilloma virus type 16 E6 and E7 oncogenes. *Proteome Sci* **7,** 29 (2009).
3. Wang, C. K., Nelson, C. F., Brinkman, A. M., Miller, A. C. & Hoeffler, W. K. Spontaneous cell sorting of fibroblasts and keratinocytes creates an organotypic human skin equivalent. *J. Invest. Dermatol.* **114,** 674–680 (2000).
4. Gratz, I. K. *et al.* Cutting edge: Self-antigen controls the balance between effector and regulatory T cells in peripheral tissues. *J. Immunol.* **192,** 1351–1355 (2014).

Figure 1

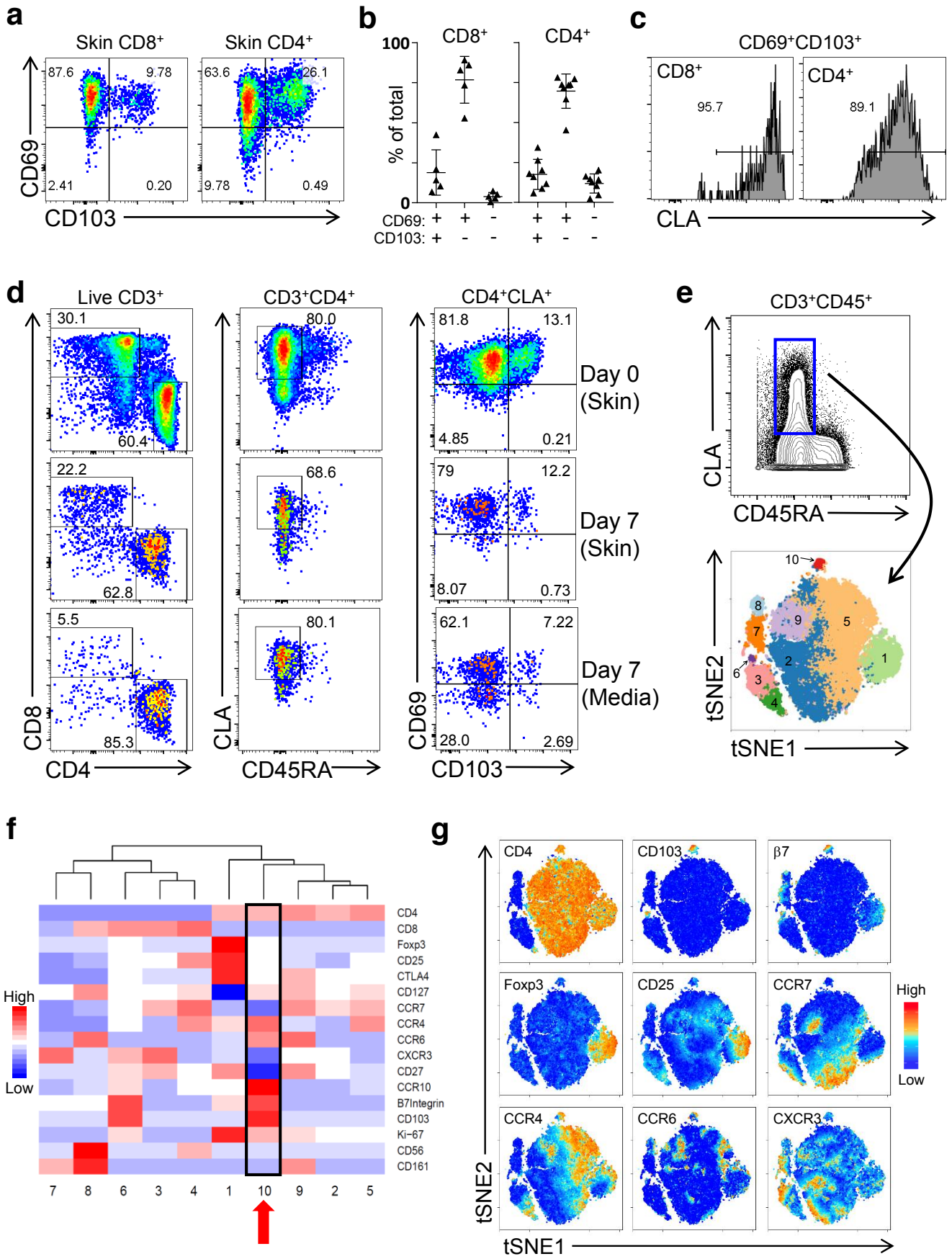
a
Skin CD8+
Skin CD4+
87.6
9.78
2.41
0.20
63.6
26.1
9.78
0.49
CD69
CD103
b
CD8+
CD4+
100
0
% of total
CD69: + + - + + -
CD103: + - - + - -
c
CD69+CD103+
CD8+
CD4+
95.7
89.1
CLA
d
Live CD3+
CD3+CD4+
CD4+CLA+
30.1
60.4
22.2
62.8
5.5
85.3
80.0
68.6
80.1
81.8
13.1
4.85
0.21
79
12.2
8.07
0.73
62.1
7.22
28.0
2.69
Day 0 (Skin)
Day 7 (Skin)
Day 7 (Media)
CD8
CD4
CLA
CD45RA
CD69
CD103
e
CD3+CD45+
CLA
CD45RA
tSNE2
tSNE1
10
8
9
5
7
2
1
6
3
4
f
High
Low
CD4
CD8
Foxp3
CD25
CTLA4
CD127
CCR7
CCR4
CCR6
CXCR3
CD27
CCR10
B7Integrin
CD103
Ki-67
CD56
CD161
7 8 6 3 4 1 10 9 2 5
g
CD4
CD103
β7
Foxp3
CD25
CCR7
CCR4
CCR6
CXCR3
High
Low
tSNE2
tSNE1

Figure 2

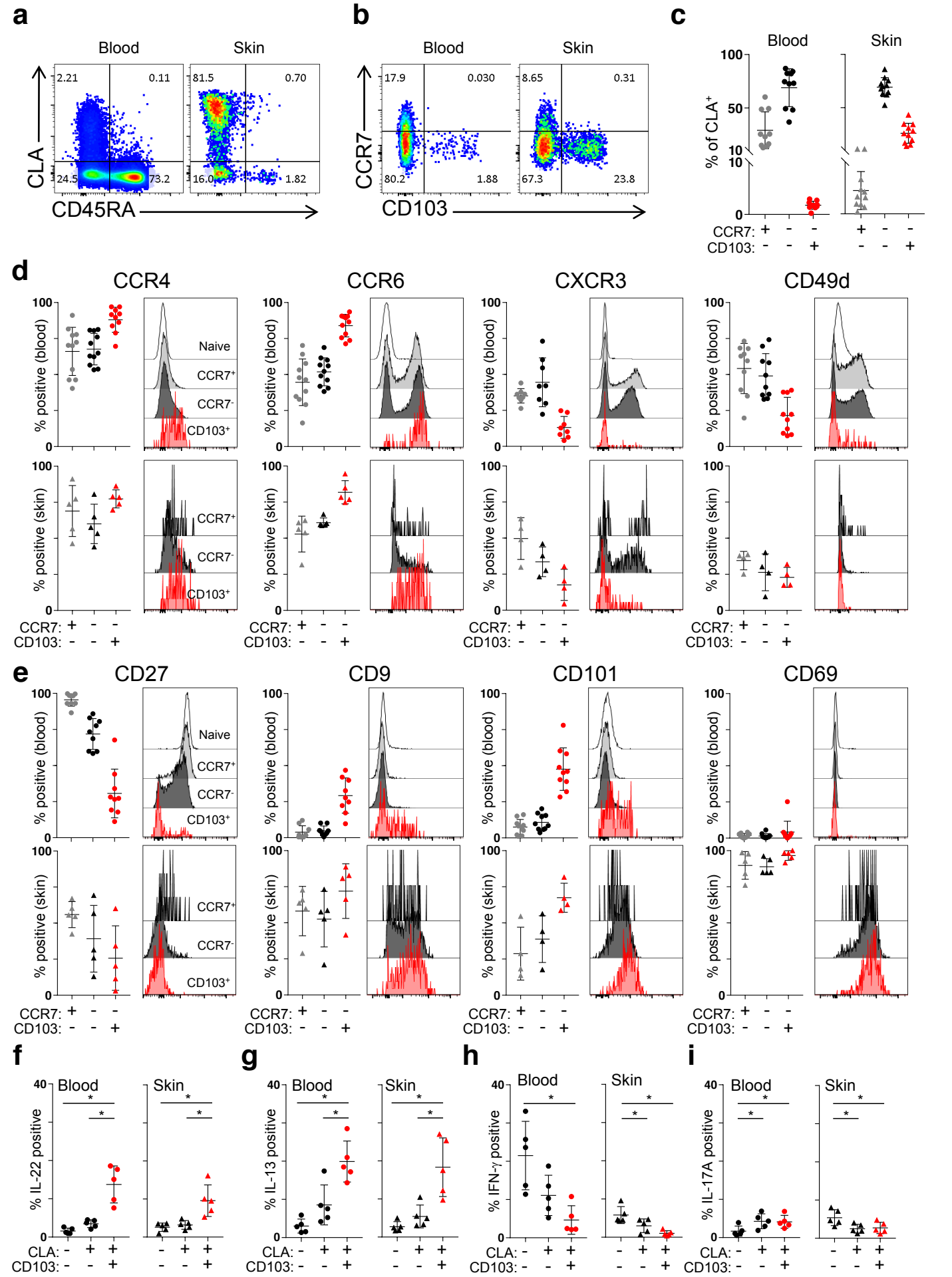
a
Blood
Skin
CLA
CD45RA
2.21
0.11
24.5
73.2
81.5
0.70
16.0
1.82
b
Blood
Skin
CCR7
CD103
17.9
0.030
80.2
1.88
8.65
0.31
67.3
23.8
c
Blood
Skin
% of CLA+
CCR7:
CD103:
d
CCR4
CCR6
CXCR3
CD49d
% positive (blood)
% positive (skin)
Naive
CCR7+
CCR7-
CD103+
e
CD27
CD9
CD101
CD69
f
g
h
i
% IL-22 positive
% IL-13 positive
% IFN-γ positive
% IL-17A positive
CLA:

Figure 3

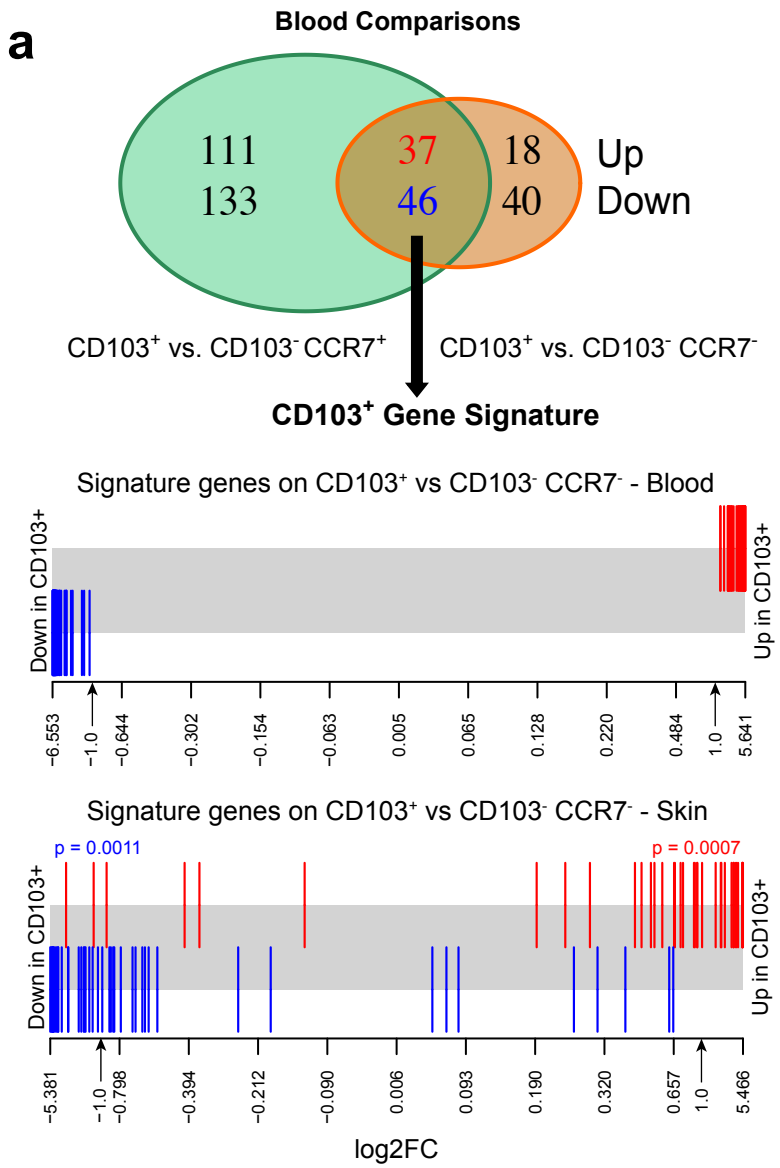
a
Blood Comparisons
111
133
37
46
18
40
Up
Down
CD103+ vs. CD103- CCR7+
CD103+ vs. CD103- CCR7-
CD103+ Gene Signature
Signature genes on CD103+ vs CD103- CCR7- - Blood
Down in CD103+
Up in CD103+
-6.553
-1.0
-0.644
-0.302
-0.154
-0.063
0.005
0.065
0.128
0.220
0.484
1.0
5.641
Signature genes on CD103+ vs CD103- CCR7- - Skin
p = 0.0011
p = 0.0007
-5.381
-1.0
-0.798
-0.394
-0.212
-0.090
0.006
0.093
0.190
0.320
0.657
1.0
5.466
log2FC

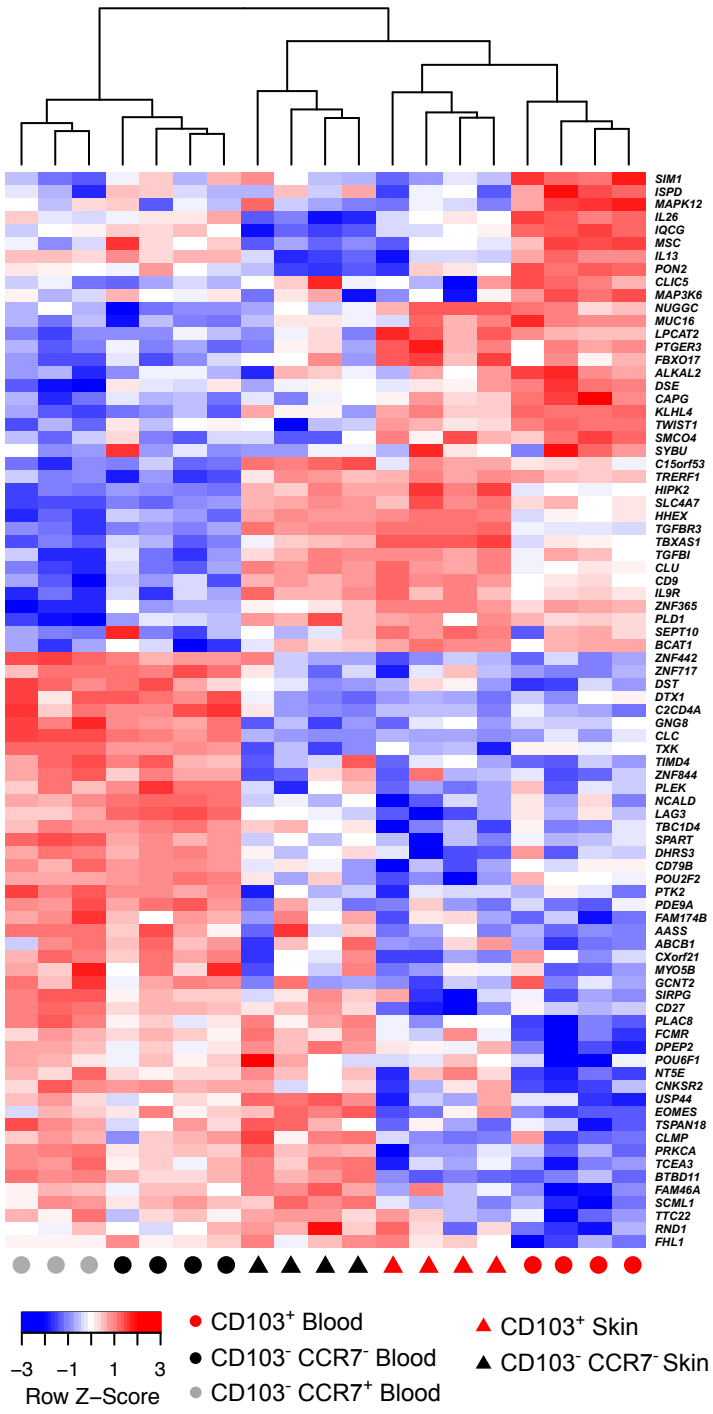
b
SIM1
ISPD
MAPK12
IL26
IQCG
MSC
IL13
PON2
CLIC5
MAP3K6
NUGGC
MUC16
LPCAT2
PTGER3
FBXO17
ALKAL2
DSE
CAPG
KLHL4
TWIST1
SMCO4
SYBU
C15orf53
TRERF1
HIPK2
SLC4A7
HHEX
TGFBR3
TBXAS1
TGFBI
CLU
CD9
IL9R
ZNF365
PLD1
SEPT10
BCAT1
ZNF442
ZNF717
DST
DTX1
C2CD4A
GNG8
CLC
TXK
TIMD4
ZNF844
PLEK
NCALD
LAG3
TBC1D4
SPART
DHRS3
CD79B
POU2F2
PTK2
PDE9A
FAM174B
AASS
ABCB1
CXorf21
MYO5B
GCNT2
SIRPG
CD27
PLAC8
FCMR
DPEP2
POU6F1
NT5E
CNKSR2
USP44
EOMES
TSPAN18
CLMP
PRKCA
TCEA3
BTBD11
FAM46A
SCML1
TTC22
RND1
FHL1
-3
-1
1
3
Row Z-Score
CD103+ Blood
CD103- CCR7- Blood
CD103- CCR7+ Blood
CD103+ Skin
CD103- CCR7- Skin

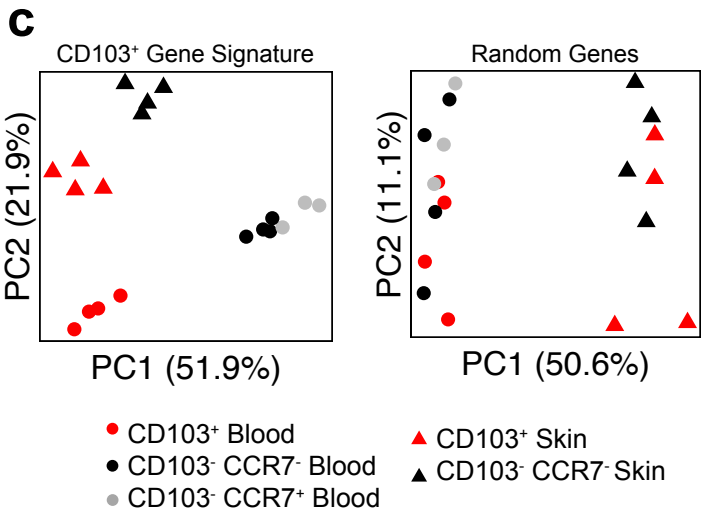
c
CD103+ Gene Signature
Random Genes
PC2 (21.9%)
PC1 (51.9%)
PC2 (11.1%)
PC1 (50.6%)
CD103+ Blood
CD103- CCR7- Blood
CD103- CCR7+ Blood
CD103+ Skin
CD103- CCR7- Skin

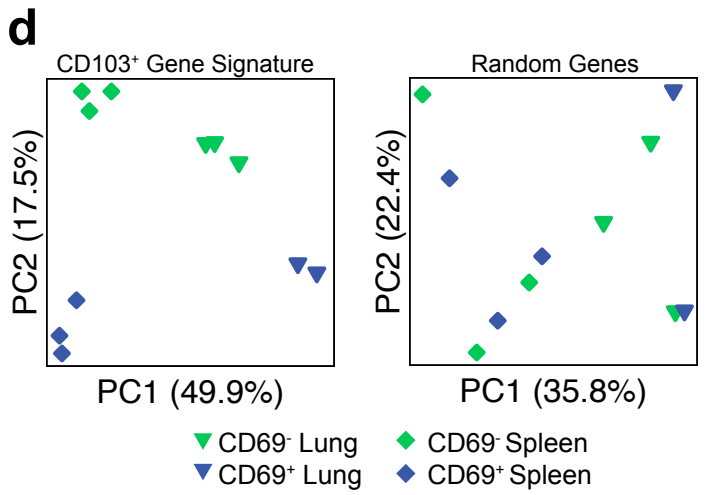
d
CD103+ Gene Signature
Random Genes
PC2 (17.5%)
PC1 (49.9%)
PC2 (22.4%)
PC1 (35.8%)
CD69- Lung
CD69+ Lung
CD69- Spleen
CD69+ Spleen

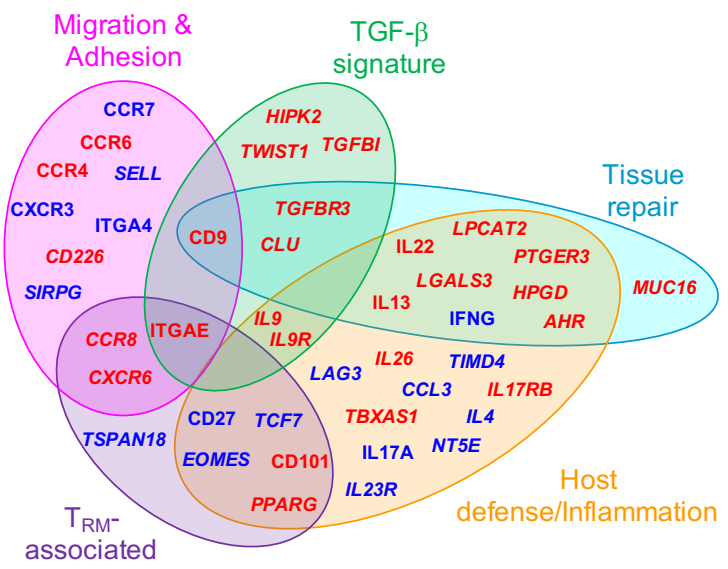
e
Migration & Adhesion
TGF-β signature
Tissue repair
Host defense/Inflammation
TRM-associated
CCR7
CCR6
CCR4
SELL
CXCR3
ITGA4
CD226
SIRPG
HIPK2
TWIST1
TGFBI
TGFBR3
CD9
CLU
LPCAT2
IL22
PTGER3
LGALS3
HPGD
MUC16
IL13
IFNG
AHR
IL9
IL9R
CCR8
ITGAE
CXCR6
LAG3
IL26
TIMD4
CCL3
IL17RB
TBXAS1
IL4
CD27
TCF7
TSPAN18
EOMES
CD101
IL17A
NT5E
PPARG
IL23R

Figure 4

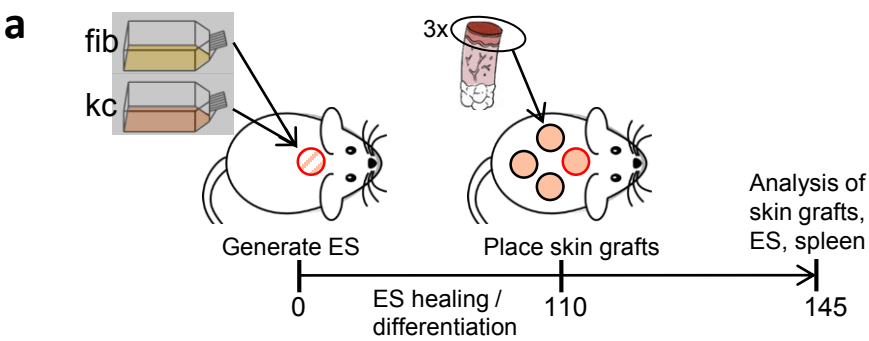
a
fib
kc
3x
Generate ES
Place skin grafts
Analysis of skin grafts, ES, spleen
0
ES healing / differentiation
110
145

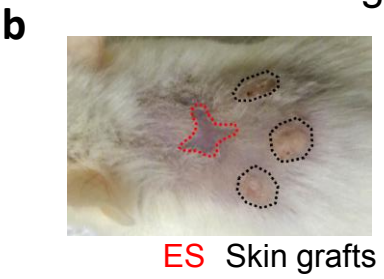
b
ES
Skin grafts

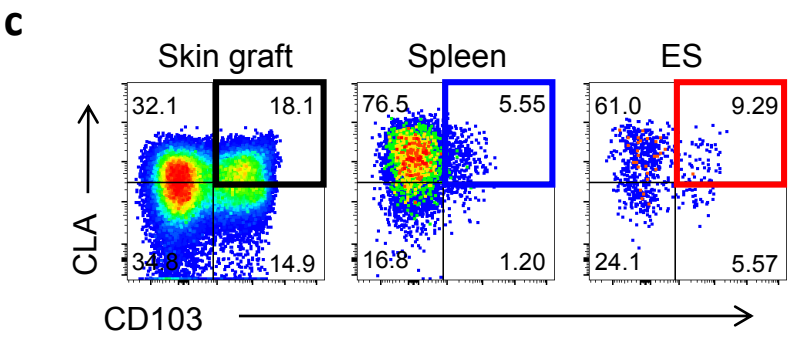
c
Skin graft
Spleen
ES
32.1
18.1
34.8
14.9
76.5
5.55
16.8
1.20
61.0
9.29
24.1
5.57
CLA
CD103

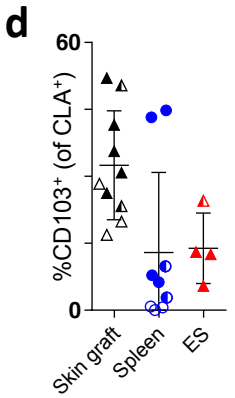
d
60
0
%CD103+ (of CLA+)
Skin graft
Spleen
ES

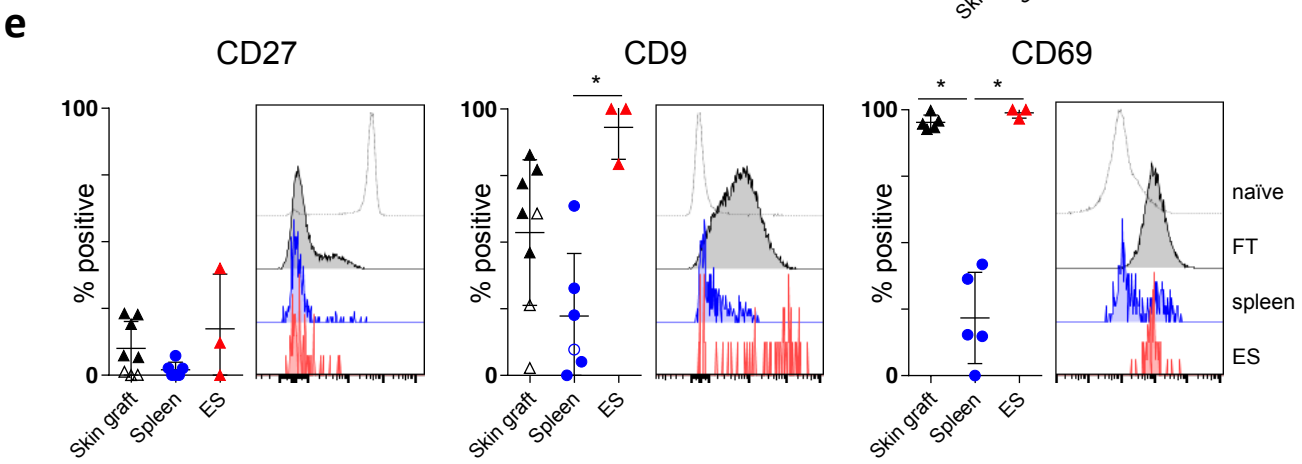
e
CD27
CD9
CD69
100
0
% positive
Skin graft
Spleen
ES
*
naïve
FT
spleen
ES

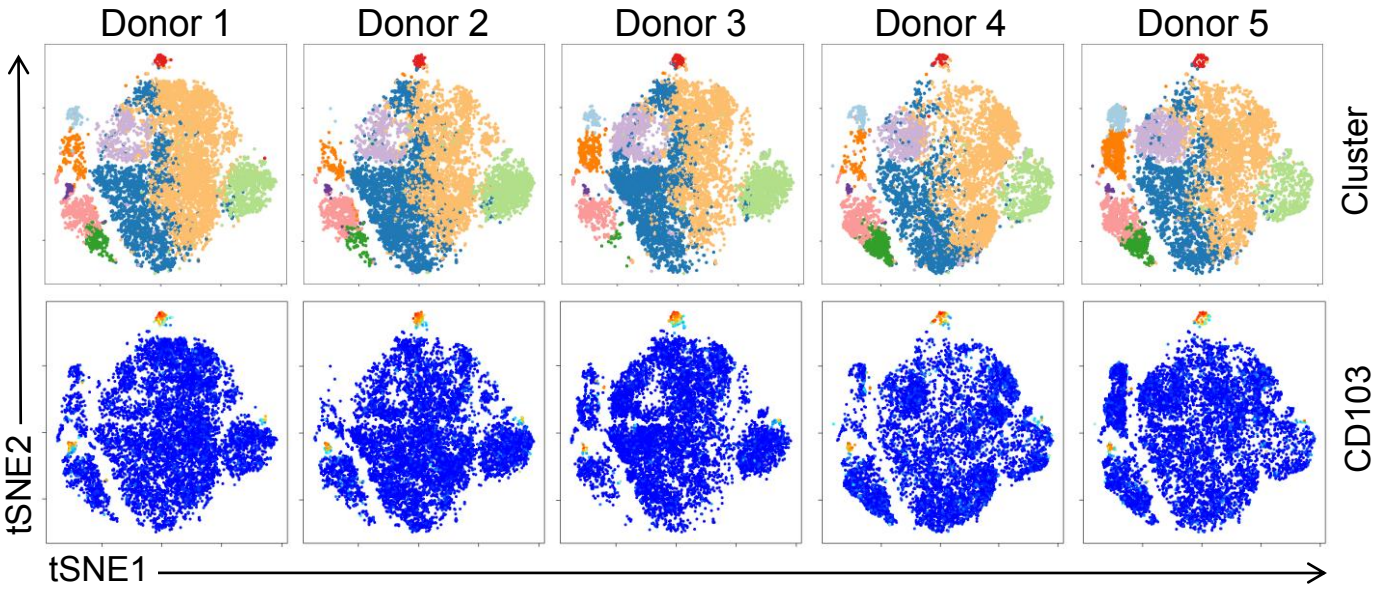

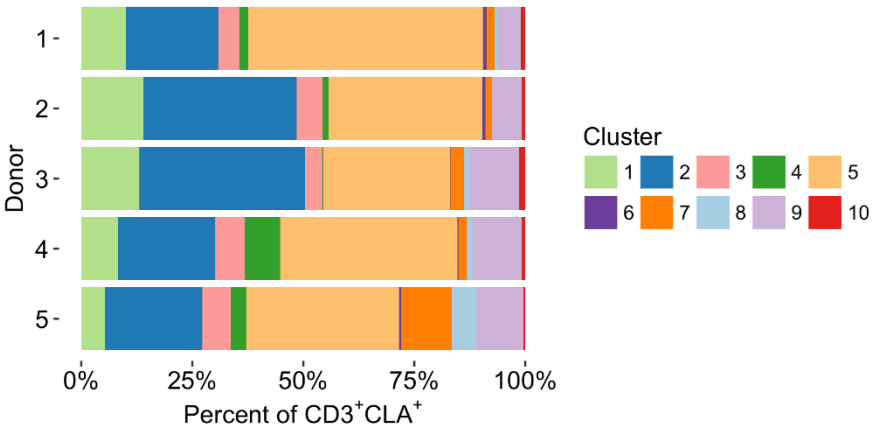

Extended Data Fig. 1: CyTOF analysis of CLA⁺ T cells in PBMC. (Top) tSNE analysis of gated $CD3^+CLA^+$ T cells from 5 individual donors showing clustering or CD103 expression as indicated. (Bottom) Stacked bar graph showing the frequency of cells in each of the 10 tSNE-defined clusters in each of the 5 donors examined.

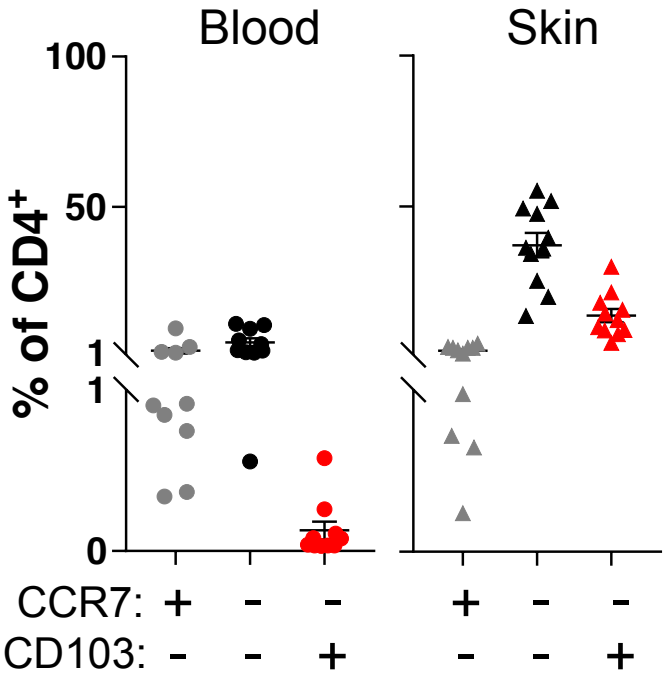

Extended Data Fig. 2: Frequencies of CLA$^+$ T cell subsets in blood and skin. Graphical summary of the proportions of CLA$^+$CCR7$^+$CD103$^-$, CLA$^+$CCR7$^-$CD103$^-$, and CLA$^+$CCR7$^-$CD103$^+$ T cells among CD4$^+$T cells from blood and skin.

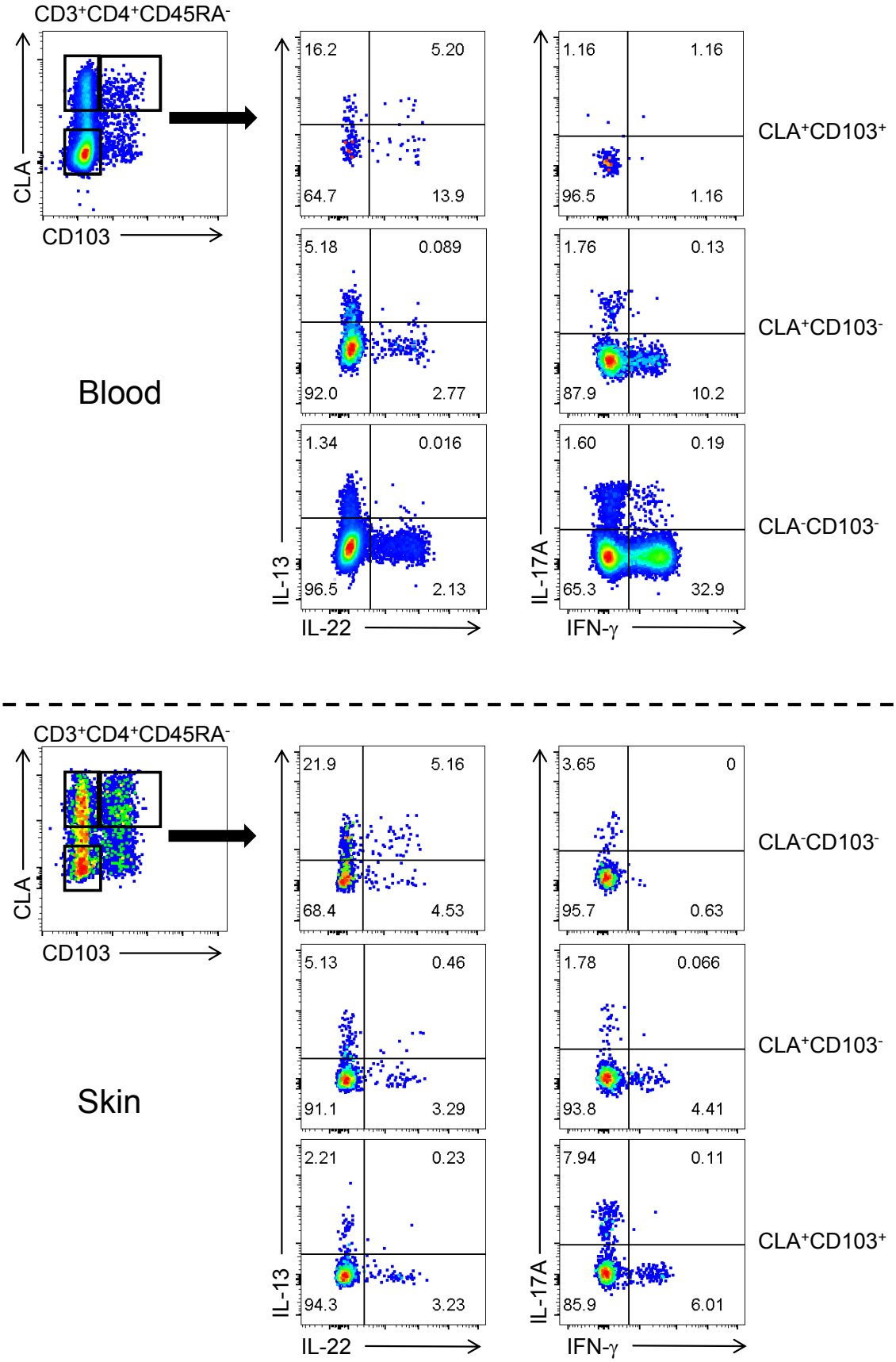

Extended Data Fig. 3: Cytokine profile of CD4+ T cells isolated from blood and skin. Representative flow cytometry analysis of IL-22, IL-13, IFN-γ, and IL-17A production by gated CLA-CD103-, CLA+CD103-, and CLA+CD103+ cells following *ex vivo* stimulation with PMA/ionomycin and intracellular cytokine staining.

a

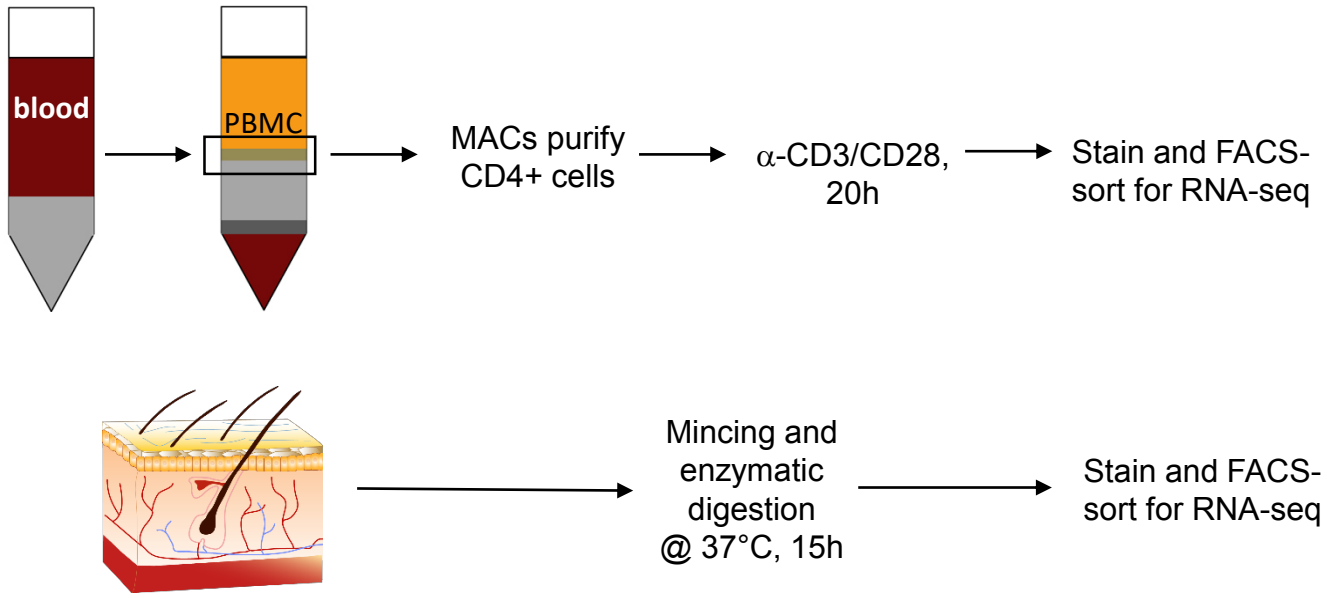

b

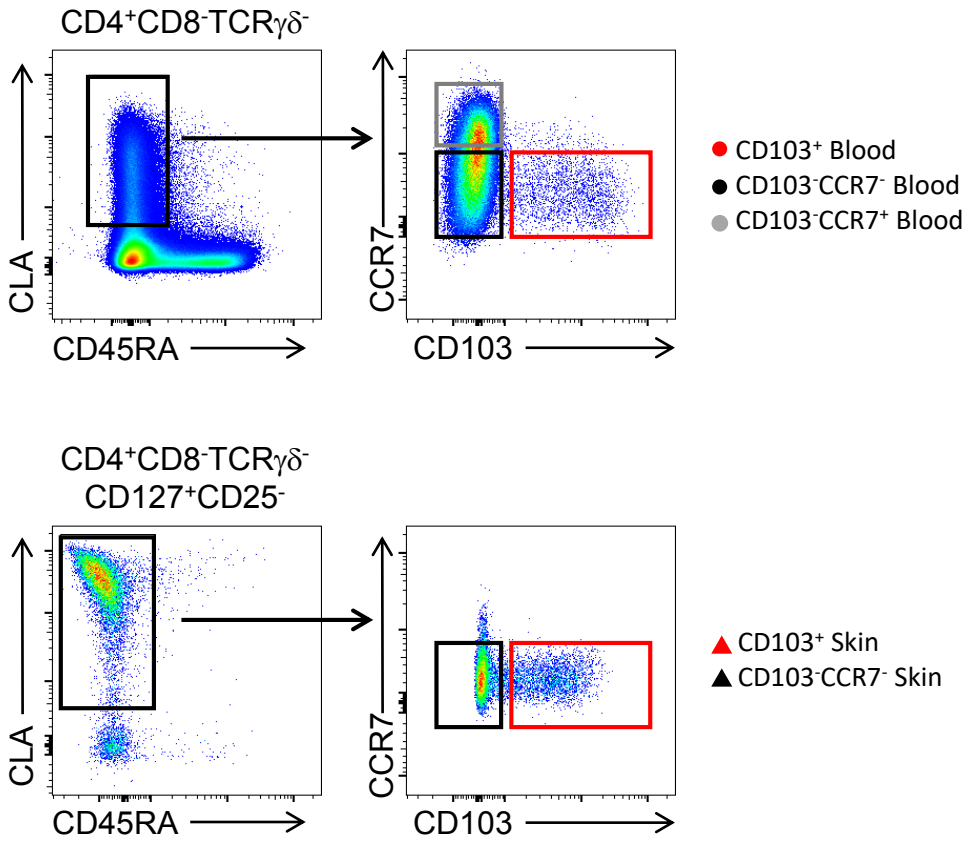

Extended Data Fig. 4: Experimental schematic of cell isolation and sort gates for RNA-seq. a, Experimental schematic for processing and sorting of T cells from blood and skin for RNA-seq analysis. **b,** Representative flow cytometry analysis of T cells isolated from blood or skin showing approximate gates used to sort the indicated populations for RNA-seq analysis.

Extended Data Figure 5

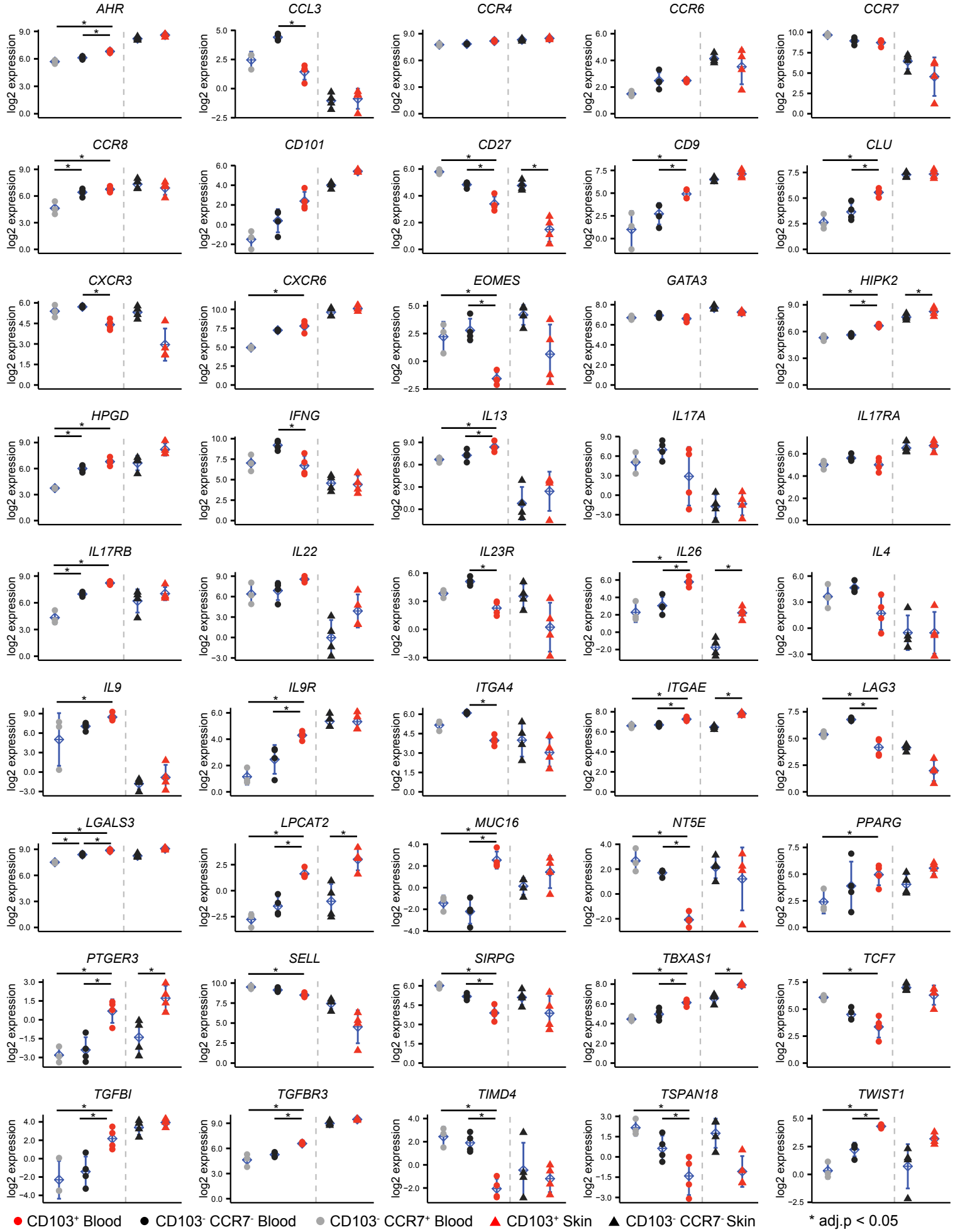

Extended Data Fig. 5. Expression of select genes in CLA⁺ T cells from skin and blood. Graphical analyses showing expression of the indicated genes in the different populations of CD4⁺CLA⁺ T cells from blood and skin as determined by RNA-seq. Adjusted p.value computed by fitting a linear model with the displayed comparisons as contrasts.

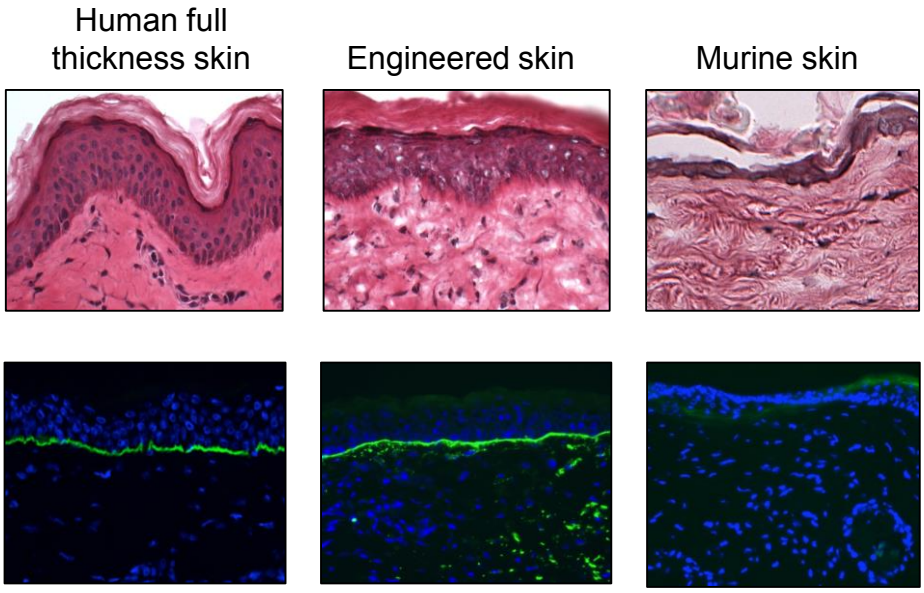

Extended Data Fig. 6: Human origin and correct differentiation of engineered skin grafts. *In vitro* expanded human keratinocytes and fibroblasts were grafted onto the backs of NSG mice using a grafting chamber. After 5 weeks of healing and differentiation, the engineered skin or adjacent murine skin were excised, frozen in OCT and stained either with hematoxylin and eosin (top) or with anti-human type VII collagen prior to immunofluorescence analysis. Human full thickness skin from a healthy donor was used as control.

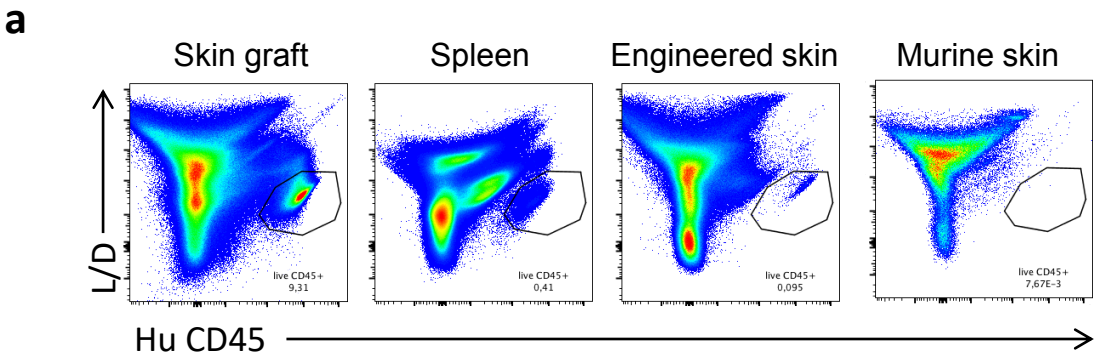

Extended Data Fig. 7: Human skin-derived cells do not infiltrate murine skin. Representative flow cytometry analysis of human CD45 expression versus live/dead stain of cells isolated from full-thickness skin graft, spleen, engineered skin, and adjacent murine skin 5 weeks after skin grafting.

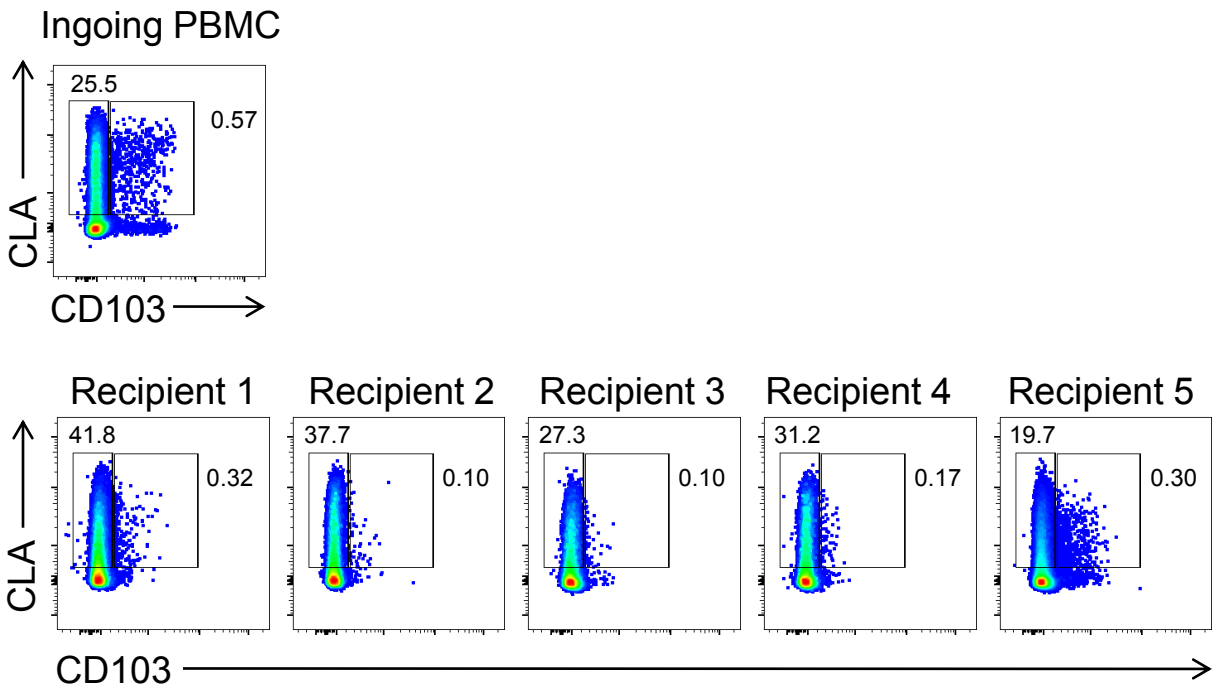

Extended Data Fig. 8: CD103 expression is not induced on human CD4⁺ T cells in NSG mice. $3x10^6$ PBMC were transferred into NSG mice and the spleens were analyzed by flow cytometry 4 weeks later. Representative flow cytometry analysis of CLA and CD103 expression by gated $CD4^+CD45RA^-$ T cells in the ingoing transferred PBMC and in cells recovered for the spleen of five individual recipients.

	Total T cell numbers	**% $CD4^+$ T cells of $CD3^+$**	**$CD103^+CLA^+$ T cells of $CD4^+$**		**% of total CLA^+CD103^+ cells**
			%	#	
Blood	1.1×10^{10}	72.13	0.13	10,314,590	**0.6**
Skin	2.04×10^{10}	57.54	13.74	1,612,823,184	**99.4**

Extended Data Table 1: $CD103^+CLA^+$ T cells in circulation constitute a minor fraction of all $CD103^+CLA^+$ T cells. Calculation of $CD103^+CLA^+$T cell numbers in skin and blood were based on total T cell numbers in these tissues as determined in reference[9], the average frequency of $CD4^+$ T cells in each tissue as determined by the investigator's labs, and the average frequency of $CD103^+CLA^+$ T cells in each tissue as shown in Extended Data Figure 2.

Extended Data Table 2

Tissue preparation

Reagent	Company	Catalog number
Collagenase Type 4	Worthington	LS004186
DNAse	Sigma-Aldrich	DN25
RPMI 1640	Gibco	31870074
human serum	Sigma-Aldrich	H5667/H4522
Penicillin/streptavidin	Sigma-Aldrich	P0781
L-Glutamine	Gibco	A2916801
NEAA	Gibco	11140035
Sodium-Pyruvat	Sigma-Aldrich	S8636
b-Mercaptoethanol	Gibco	31350-010
PBS	Gibco	14190169
Ficoll Paque Plus	GE-Healthcare	GE17-1440-02

Cellular activation

Reagent	Company	Catalog number
CD4 microbeads	Miltenyi	130-045-101
Immuno Cult Human CD3/CD28 T cell activator	Stemcell Technologies	10971
PMA	Sigma-Aldrich	P8139
Ionomycin	Sigma-Aldrich	I06434
Brefeldin A	Sigma-Aldrich	B6542
Cytofix/Cytoperm kit	BD	RUO 554714
Recombinant human IL-2	Immunotools	11340023

Skin cell culture and transplantation

Reagent	Company	Catalog number
Epilife	Gibco	MEPICF500
DMEM	Gibco	11960-044
MEM	Gibco	11380037
TrypLE express	Gibco	12604021
Primocin	invitrogen	ant-pm-1
Histoacryl	BRAUN	1050044

Tissue preparation from mice

Reagent	Company	Catalog number
BD Pharm Lyse	BD	555899
Collagenase from Clostridium histolyticum	Sigma-Aldrich	C9407
Hyaluronidase	Sigma-Aldrich	H3506

CyTOF

Reagent	Company	Catalog number
PBS (Ca and Mg free)	Sigma	D8537
Cisplatin, 100 mM in DMSO	Enzo Life Sciences	ALX-400-040-M250
Human TruStain FcX	BioLegend	422302
MaxPar Nuclear Antigen Staining Buffer Set	Fluidigm	201063
MaxPar Fix and Perm Solution	Fluidigm	201067
Cell-ID Intercalator-Ir, 125 uM (500X)	Fluidigm	201192A
MaxPar EQ Four Element Calibration Beads	Fluidigm	201078

Histology

Reagent	Company	Catalog number
TissueTek	Hartenstein	TTEK
Hemalum solution acid acc. to Mayer	Carl Rorth	T865.1
Eosin Y aqueous solution	Sigma	HT110232
ProLong™ Gold Antifade Mountant with DAPI	Invitrogen	P36931

Antibodies

Reagent	Company	Catalog number
CD103 FITC (B-Ly7)	eBioscience	11-1038-42
CCR4 PerCP-Cy5.5 (L291H4)	Biolegend	359406
CCR8 PE (L263G8)	Biolegend	360604
CD45RA PE-e610 (HI100)	eBioscience	61-0458-42
CD3 PE-Cy5.5 (UCHT1)	eBioscience	15-0038-42
CCR6 PE-Cy7 (R6H1)	eBioscience	25-1969-42
CD4 Alexa Fluor 700 (RPA-T4)	Biolegend	300526
Fixable Viability Dye eFluor® 780	eBioscience	65-0865-14
CXCR3 bv421 (1C6/CXCR3)	BD	562558
CLA bv605 (HECA-452)	BD	563960
IL-17A PerCP-Cy5.5 (eBio64DEC17)	eBioscience	45-7179-42
IL-13 PE (JES10-5A2)	BD	554571
IL-22 PE-Cy7 (22URTI)	eBioscience	25-7229-42
GM-CSF bv421 (BVD2-21C11)	BD	562930
CD8 Pacific Orange (3B5)	eBioscience	MHCD0830
IFN-g BV605 (4S.B3)	BD	563731
CLA FITC (HECA-452)	Biolegend	321306
TCRgd PerCP-eFluor710 (B1.1)	eBioscience	46-9959
CD3 PE (HIT3a)	BD	561803
CD4 PE-594 (RPA-T4)	Biolegend	300548
CD25 PE-Cy7 (BC96)	eBioscience	302612
CD103 APC (Ber-ACT8)	Biolegend	350216
CD45RA Alexa Fluor 700 (HI100)	Biolegend	304120
CD127 bv 421 (HIL-7R-M21)	BD	560823
CD8 bv510 (RPA-T8)	Biolegend	301048

CCR7 bv605 (G043H7)	Biolegend	353224
CD101 PerCP-Cy5.5 (BB27)	Biolegend	244438
CD9 PE (M-L13)	BD	341647
CD69 BV605 (FN50)	Biolegend	310938
CD45 BV785 (HI30)	Biolegend	304048
CD3 BV421 (UCHT1)	Biolegend	300434
CCR6 PE-Cy7 (G034E3)	Biolegend	353418
CD27 PE-594 (M-T271)	BioLegend	356422
CD4 PE-Cy5 (RPA-T4)	BioLegend	300510
CD27 BV711 (M-T271)	BioLegend	356430
CD127 PE-Cy7 (A019D5)	BioLegend	351320
CCR7 bv421 (G043H7)	BioLegend	353232
CD8 bv785 (RPA-T8)	BioLegend	301046
IF primary antibody: rabbit anti-human NC-1 domain of type VII collagen (LH7.2)	kindly provided by Dr. Alexander Nyström, University of Freiburg, Germany	
IF secondary antibody: goat anti-rabbit A488	ThermoFisher	A11008

Antibodies for CyTOF

Reagent	Company	Catalog number
CLA FITC (HECA-452)	BioLegend	321306
Integrin-beta7 APC (FIB504)	BioLegend	321208
CTLA4 147Sm (14D3)	Fluidigm	Custom
Ki-67 161Dy (B56)	Fluidigm	3161007B
Foxp3 162Dy (259D/C7)	Fluidigm	3162024A
CCR6 141Pr (G034E3)	Fluidigm	3176022A
CD19 142Nd (HIB19)	Fluidigm	3142001B
CD123 143Nd (6H6)	Fluidigm	3143014B
CD38 144Nd (HIT2)	Fluidigm	3144014B
CD4 145Nd (RPA-T4)	Fluidigm	3145001B
IgD 146Nd (IA6-2)	Fluidigm	3146005B
CD16 148Nd (3G8)	Fluidigm	3148004B
CCR4 149Sm (205410)	Fluidigm	3149029A
CD103 151Eu (Ber-ACT8)	Fluidigm	3151011B
CD45RO 152Sm (UCHL1)	Fluidigm	Custom
CD45RA 153Eu (HI100)	Fluidigm	3153001B
CD45 154Sm (HI30)	Fluidigm	3154001B
CD27 155Gd (M-T271)	Fluidigm	3155001B
CXCR3 156Gd (1C6)	Fluidigm	3156004B
CD10 158Gd (HI10a)	Fluidigm	3158011B
CD161 159Tb (HP-3G10)	Fluidigm	3159004B
CD14 160Gd (M5E2)	Fluidigm	3160001B
Anti-APC 163Dy	Fluidigm	3163001B
CCR0 164Dy (314305)	Fluidigm	Custom
CD127 165Ho (A019D5)	Fluidigm	3165008B
CD24 166Er (ML5)	Fluidigm	3166007B
CCR7 167Er (150503)	Fluidigm	3167009A
CD8 168Er (SK1)	Fluidigm	3168002B
CD25 169Tm (M-A251)	Fluidigm	3169003B
CD3 170Er (UCHT1)	Fluidigm	3170001B
IgM 172Yb (MHM-88)	Fluidigm	3172004B
HLA-DR 173Yb (L243)	Fluidigm	3173005B
Anti-FITC 174Yb	Fluidigm	3174006B
CRTh2 175Lu (BM16)	Fluidigm	Custom
CD56 176Yb (HCD56)	Fluidigm	3176001B